Analytical Evaluation of Transmission Penalty Due to Group Velocity Dispersion, Self-Phase Modulation, and Amplifier Noise in Optical Heterodyne CPFSK Systems

B. Pal, R. Gangopadhyay, and G. Prati

***Abstract*—An analytical bit error rate evaluation of an optical heterodyne continuous-phase frequency shift keying (CPFSK) transmission system affected by group-velocity dispersion (GVD), self-phase modulation (SPM), and erbium-doped fiber amplifier (EDFA) amplifier spontaneous emission noise (ASE) in a nonlinear fiber medium is carried out following a perturbative and a transfer matrix approach. The utility of both approaches has been exemplified by applying them to different dispersion compensation schemes in optical and electronic domains. The theoretical penalty estimates are found to have good agreement with both the reported experimental results and those obtained by the Q-value simulation.**

***Index Terms*—Coherent optical system, dispersion compensation (DC), matrix analysis, nonlinear effects, transmission penalty.**

I. Introduction

THE USE of high power as well as high bit rate operation to achieve higher capacity and longer transmission distance in an optically amplified single mode fiber (SMF) communication system is significantly limited by attendant group velocity dispersion (GVD), the GVD induced self-phase modulation (SPM) and the accumulated amplifier spontaneous emission (ASE) noise of the optical amplifier. In case of intensity modulated direct detection (IM–DD) optical transmission, the transmission penalty due to the combined effect of GVD and SPM can be determined theoretically [1] in terms of the change in root-mean square pulse width of an optical pulse after nonlinear fiber transmission without optical repeater. In the presence of optical repeaters, an approximate analytical technique is provided to quantify the nonlinear waveform distortion in terms of an equivalent increase of the transmitter α parameter [2] as a measure of the attendant frequency chirping. These theoretical evaluation techniques although provide better qualitative and quantitative understanding of the underlying nonlinear mechanism than can be available from the numerical split step Fourier (SSF) method [3], they lack accuracy at higher operating power level.

Manuscript received February 16, 1999; revised December 10, 1999. This work was supported for this this project was provided by the European Community, Brussels.

B. Pal and R. Gangopadhyay are with the Indian Institute of Technology, Kharagpur, India (e-mail: ranjan@ece.iitkgp.ernet.in).

G. Prati is with the Department of Information Engineering, University of Parma, Parma I-43100, Italy.

Publisher Item Identifier S 0733-8724(00)03027-9.

In a medium-haul repeatered transmission link the coherent systems enjoy advantages compared to IM–DD systems in respect of repeater spacing and the required repeater optical output power [4]. Further, the coherent system allows efficient dispersion compensation at the IF domain [4] and narrow channel spacing for WDM systems. For an optically repeatered transmission system employing angle modulated signals such as phase-shift keying (PSK), differential phase-shift keying (DPSK), continuous-phase frequency shift keying (CPFSK), etc., the penalty due to the combined effect of GVD, SPM, and ASE noise is mostly assessed by numerical SSF method [5] or by semianalytical approach [6]. A more exact analytical technique for the evaluation of the performance penalty for coherent angle-modulated systems in nonlinear fiber transmission medium is therefore needed. In this paper we carry out an analytical evaluation of the penalty due to GVD, SPM, and ASE noise for an angle modulated system using perturbation and matrix analysis approach by invoking the results of the linear phase approximation to a linearly filtered angle modulated signal [7], [8]. The analysis is valid not only for random nonreturn-to-zero (NRZ) data but can also accommodate various line coding schemes as well as different dispersion compensation schemes aimed at reducing the overall penalty.

II. Theoretical Analysis

A. Linear Phase Approximation

If an angle-modulated signal $A(t)e^{[j\phi(t)]}$, where $A(t)$ is the signal envelope and $\phi(t)$ is the angle modulation, is input to a linear system with its low-pass equivalent impulse response $h(t)$, [$h(t)$ can be complex], the output phase $\theta(t)$ and the envelope $a(t)$ can be obtained as [7]–[9]

$$\theta(t) = \mathrm{Re}[h(t) \otimes \Psi(t)] + \sum_{n=2,\,\infty} \frac{1}{n!}\,\mathrm{Im}[j^n f_n(t)] \quad (1)$$

$$\log[a(t)] = -\mathrm{Im}[h(t) \otimes \Psi(t)] + \sum_{n=2,\,\infty} \frac{1}{n!}\,\mathrm{Re}[j^n f_n(t)] \quad (2)$$

where $\mathrm{Re}(.)$ and $\mathrm{Im}(.)$ denote the real and imaginary part of the argument, respectively, $\Psi(t) = \phi(t) - j\,\log\,A(t)$, and the exact expression of $f_n(t)$ is available in [7]. Equations (1) and (2) assume that the complex variables $A(t)^{[j\phi(t)]}$ and $h(t)$ are homomorphic, i.e., all higher order derivatives of $\phi(t)$, $A(t)$, and $h(t)$ exist. If the $\lim_{t\to\infty} h(t)$ converges quickly, then the nonlinear distortion terms $\sum_{n=2}^{\infty}(1/n!)\mathrm{Im}[j^n f_n(t)]$ also converge quickly [7]. Under this assumption, and defining $h_r(t) = \mathrm{Re}\{h(t)\}$ and $h_i(t) = \mathrm{Im}[h(t)]$ and taking the first-order linear terms, (1) and (2) can be simplified in the following form:

$$\theta(t) = h_i(t) \otimes \log A(t) + h_r(t) \otimes \phi(t) \tag{3}$$

$$\log[a(t)] = h_r(t) \otimes \log A(t) - h_i(t) \otimes \phi(t). \tag{4}$$

If A_m is the mean value of either $a(t)$ or $A(t)$ and the average power fluctuation $\Delta s_{\mathrm{out}}(t) = 2\Delta a(t) A_m$ or $\Delta s_{\mathrm{in}}(t) = 2A_m \Delta A(t)$ where $\Delta a(t)$ and $\Delta A(t)$ are the corresponding envelope fluctuations about A_m, $\log(A(t))$ and $\log(a(t))$ can be redefined in the following way:

$$\log[A^2(t)] \approx \log A_m^2 - 1 + \frac{\Delta s_{\mathrm{in}}(t)}{A_m^2} \tag{5}$$

$$\log[a^2(t)] \approx log A_m^2 - 1 + \frac{\Delta s_{\mathrm{out}}(t)}{A_m^2}. \tag{6}$$

Substituting (5) and (6) in (3) and (4), we obtain

$$\frac{\Delta s_{\mathrm{out}}(t)}{2A_m^2} \approx \frac{1}{2A_m^2} \Delta s_{\mathrm{in}}(t) \otimes h_r(t) - \phi(t) \otimes h_i(t) \tag{7}$$

$$\theta(t) \approx \frac{1}{2A_m^2} \Delta s_{\mathrm{in}}(t) \otimes h_i(t) + \phi(t) \otimes h_r(t). \tag{8}$$

Defining $h(t) = F^{-1}[\exp(-jF(\omega)]$ where F denotes the Fourier transform and $\langle S \rangle = A_m^2$, a direct frequency domain transform of (7) and (8) leads to the following matrix representation [9]:

$$\begin{pmatrix} \phi_{\mathrm{out}}(\omega) \\ \zeta_{\mathrm{out}}(\omega) \end{pmatrix} = \boldsymbol{D}(\omega) \begin{pmatrix} \phi_{\mathrm{in}}(\omega) \\ \zeta_{\mathrm{in}}(\omega) \end{pmatrix} \tag{9}$$

where $\zeta(\omega)$ and $\phi(\omega)$ are the Fourier transform of $\Delta S(t)$ and $\phi(t)$, respectively, and

$$\boldsymbol{D}(\omega) = \begin{pmatrix} \cos(F(\omega)) & \dfrac{\sin(F(\omega))}{2\langle S \rangle} \\ -2\langle S \rangle \sin(F(\omega)) & \cos(F(\omega)) \end{pmatrix}. \tag{10}$$

For a dispersion limited fiber link $F(\omega) = \frac{1}{2}\beta_2 z \omega^2$, where $\beta_2 = -(\lambda_c^2 D_c / 2\pi c)$, D_c is the dispersion coefficient, c is the velocity of light in vacuum, λ_c is the wavelength of the transmitting laser and z is the fiber length. Interestingly, (10) has also been obtained in the past by small signal analysis [10]. Equation (9) establishes the relationship between the input vector $\xi_{\mathrm{in}}(\omega) = [\phi_{\mathrm{in}}(\omega), \zeta_{\mathrm{in}}(\omega)]$ and the output vector $\xi_{\mathrm{out}}(\omega) = [\phi_{\mathrm{out}}(\omega), \zeta_{\mathrm{out}}(\omega)]$ in a dispersion limited fiber link.

In the absence of GVD and considering only the effect of third-order Kerr nonlinearity, the relationship between the input vector and the output vector can be written as

$$\xi_{\mathrm{out}}(\omega) = \boldsymbol{N}(z, \omega) \xi_{\mathrm{in}}(\omega) \tag{11}$$

with

$$N(z, \omega) = \begin{pmatrix} 1 & 0 \\ \gamma z & 1 \end{pmatrix} \tag{12}$$

where γ is the nonlinear coefficient. Note, that $\phi_{\mathrm{out}}(\omega)$ implicit in (11) is defined as the Fourier transform of the fluctuation part of the phase only and which does not include the constant phase induced by the constant power level.

For a propagating angle-modulated signal the nonlinear effect arises from the SPM due to GVD induced PM–AM conversion, which means that the noncommuting operators $D(z, \omega)$ and $\boldsymbol{N}(z, \omega)$ are acting simultaneously. Hence, utilizing the Baker–Hausdorff relation of the noncommuting operators [11], a first-order approximation of the input–output phase relationship can be established using (9) and (11)

$$\xi_{\mathrm{out}}(\omega) = \boldsymbol{N}(z, \omega)\boldsymbol{D}(z, \omega)\xi_{\mathrm{in}}(\omega) + [\boldsymbol{o}(z)]\xi_{\mathrm{in}}(\omega) \tag{13}$$

where

$$\boldsymbol{o}(z) = \tfrac{1}{2}[\boldsymbol{N}(z, \omega), \boldsymbol{D}(z, \omega)] + \tfrac{1}{12}[\boldsymbol{N}(z, \omega) - \boldsymbol{D}(z, \omega), [\boldsymbol{N}(z, \omega), \boldsymbol{D}(z, \omega)]] \tag{14}$$

with the commutation bracket

$$[\boldsymbol{N}(z, \omega), \boldsymbol{D}(z, \omega)] = \boldsymbol{N}(z, \omega)\boldsymbol{D}(z, \omega) - \boldsymbol{D}(z, \omega)N(z, \omega).$$

Based on (13), two analytical methods have been developed for the purpose of representing a nonlinear fiber influenced by GVD and SPM by a linearized system described by an equivalent impulse response for facilitating system analysis. In the first method, we have utilized the fact that for small $F(\omega)$, $\boldsymbol{o}(z) \approx [\boldsymbol{N}(z, \omega), \boldsymbol{D}(z, \omega)]$, and following a perturbative approach to evaluate the error due to the higher order terms like $[\boldsymbol{N}(z, \omega), [\boldsymbol{N}(z, \omega), \boldsymbol{D}(z, \omega)]]$ to find out an impulse response of the system affected by GVD induced SPM. In the recent past the similar approaches that have been employed [1], [2], [12] to quantify the transmission penalty of the IM–DD systems, although merit simplicity and computational efficiency, suffer a large inaccuracy as the nonlinear effect increases. Due to these difficulties, we have also developed a more accurate transfer matrix method, utilizing the fact that $\lim_{z\to 0} \boldsymbol{o}(z) = 0$.

B. Perturbation Method

In this section we follow an analysis similar to the time dependent perturbation theory in Quantum mechanics [13]. The nonlinear Schroedinger equation (NLS) in frequency domain is given by [3]

$$j\,\frac{\partial U(z, \omega)}{\partial z} = \frac{\beta_2 \omega^2}{2} U(z, \omega) - \gamma U'(z, \omega) U(z, \omega) \tag{15}$$

where $U(z, \omega)$ and $U'(z, \omega)$ are the Fourier transforms of the signal envelope $A(t)e^{\phi(t)}$ and $|A(t)|^2$, respectively, at a distance z. In the framework of linear phase approximation (9), and in the absence of nonlinearity, we introduce an evolution operator for the phase spectrum

$$A_D(L, 0, \omega) = \exp\left[\int_{z=0}^{L} H(z, \omega)\, dz\right] = \exp\left[-j\,\frac{\beta_2 \omega^2}{2}\, L\right]. \tag{16}$$

This operator is similar to the evolution operator of the zeroth-order Hamiltonian $H_0(\omega) = \beta_2\omega^2/2$.

In the absence of nonlinearity using (10) $U'(z, \omega)$ can be expressed as

$$U'(z, \omega) = P_o e^{-\alpha z}\delta(\omega) - 2P_o e^{-\alpha z} \sin[F(z, \omega)]\phi(0, \omega) \tag{17}$$

where, $\phi(0, \omega)$ is the Fourier transform of the fluctuating part of the phase $\phi(t)$ at $z = 0$ and $P_0 = \langle S \rangle$ and α is the attenuation constant of the fiber. Incorporating (17) in (15) we rewrite (15) as

$$j\,\frac{\partial U(z, \omega)}{\partial z} = \left[\frac{\beta_2\omega^2}{2} - 2P_o e^{-\alpha z} \sin[F(z, \omega)]\phi(0, \omega)\right] \cdot U(z, \omega). \tag{18}$$

The total Hamiltonian of the system represented by (18) is

$$H(z, \omega) = H_0(\omega) + \Delta H(\omega, z) \tag{19}$$

where

$$\Delta H(\omega, z) = 2\gamma P_o e^{-\alpha z} \sin[F(z, \omega)]\phi(0, \omega) \tag{20}$$

and the total evolution operator of the system is expressed as

$$A(z, 0, \omega) = A_D(z, 0, \omega)A_N(z, 0, \omega). \tag{21}$$

The evolution of $A_N(z, 0, \omega)$ in differential form is given as

$$\frac{dA_N(z, \omega)}{dz} = \Delta H_I(\omega, z)A_N(z, \omega) \tag{22}$$

where $\Delta H_I(\omega, z) = A_D^{-1}(z, 0)\Delta H(\omega, z)A_D(z, 0)$. The solution of (22) over a fiber length L is given by the following perturbation series:

$$\begin{aligned} &A_N(L, 0, \omega) \\ &= 1 + \int_{z=0}^{L} \Delta H(\omega, z)\,dz + \int_{z=0}^{L} dz \int_{z'=0}^{z} \\ &\quad \cdot \Delta H_I(\omega, z')\Delta H_I(\omega, z')A_N(z', 0, \omega)\,dz' + \cdots. \end{aligned} \tag{23}$$

This series convergence depends on the convergence of (13). In order to establish an approximate linearized model of a nonlinear fiber we retain the first two terms of (23). Recognizing $A_D(L, \omega)A_N(L, \omega)$ as the approximated transfer function of the fiber and applying linear phase approximation mentioned in Section II-A [cf., (1) and (2)] ,one can obtain the fluctuating part of the output phase $\phi(L, t)$ after some algebraic manipulation as

$$\phi(L, t) = \mathrm{Re}\big[F^{-1}[H_{DS}(L, \omega)\phi(0, \omega)]\big] \tag{24}$$

where

$$H_{DS}(L, \omega) = A_D(L, 0, \omega)A_N(L, 0, \omega) \tag{25}$$

with

$$A_N(L, 0, \omega) = 1 + 2P_o\gamma I(L, \omega) \tag{26}$$

where the function $I(z, \omega)$ is expressed as

$$I(z, \omega) = \frac{\beta}{\alpha^2 + \beta^2} - \frac{e^{-\alpha z}}{\sqrt{\alpha^2 + \beta^2}} \sin\left[\beta z + \tan^{-1}\left(\frac{\beta}{\alpha}\right)\right] \tag{27}$$

and $\beta = [\beta_2\omega^2]/2$.

A physical interpretation of (25) can be appreciated from the following discussion.

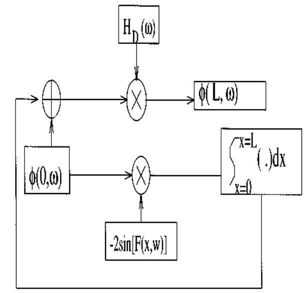

Fig. 1. Perturbation diagram in the first-order approximation.

The Fourier transform of (25) the induced SPM phase due to PM–AM conversion at a distance L' is given by

$$\Delta\phi_{\mathrm{SPM}}(\omega) = \gamma \int_{z=0}^{L'} U'(z, \omega)\,dz. \tag{28}$$

According to the interpretation of the first-order term in (23), this SPM phase (evaluated at $L' = L$) is added with the input phase and the resultant complex envelope is allowed to pass through the linear fiber having suffered GVD alone (see Fig. 1). Applying linear phase approximation, we obtain the output phase as obtained in (24).

Equation (24) provides excellent results for a meaningful range of input power but at high operating power level, (24) does not hold good because of the omission of the higher order correction terms in (23). These higher order terms were ignored in order to establish a linear relationship between the input phase and output phase for the purpose of modeling the system linearly. However, a heuristic approach can reduce the mean-square error (mse) between the simulated phase and the theoretically obtained phase at high power. While Kikuchi worked with $L' = L$, we postulate that the SPM phase that is being added at the beginning is to be evaluated at a suitable length L' instead of L and the choice of L' will depend on the relative strength of the GVD and SPM effect. A simplest way of doing it is to set $L' = k'(L_{NL}/L_D)L$, $L_{NL} = L/\gamma P_o L_{\mathrm{eff}}$, where $L_{\mathrm{eff}} = (1 - e^{-\alpha L})/\alpha$, $L_D = (\beta_2 R^2)^{-1}$, R is the data rate and k' is chosen by comparison of the result of simulation so as to minimize the mse. It was found that $k' = 2$ is a very good choice over a significant range of optical power level. Though this method yields good results, but for its heuristic nature we develop a theoretically more accurate matrix method for the evaluation of the impulse response of a nonlinear fiber in Section II-E that holds good even at high operating power levels.

C. Analysis of Multisegment Link by Perturbation Method

In a cascaded, multisegment optical link, the relationship between the Fourier transform of the phase at the end of the Nth and $(N-1)$th segment is given by

$$\begin{aligned} \phi_N(L_N, \omega) = &H_{DS}^{(N)}(L_N, \omega)\phi_{N-1}(L_{N-1}, \omega) \\ &+ 2H_D^{(N)}(L_N, \omega)\gamma P_0\chi(N-1, \omega) \end{aligned} \tag{29}$$

where $H_{DS}^{(N)}(.)$ represents the equivalent transfer function which accounts for the GVD induced SPM in the Nth segment and L_N is the length of the Nth segment. Assuming, that the amplifier exactly compensates the loss in each segment, the Fourier transform of the SPM phase that has been induced from the beginning of the Nth segment to the length L'_N due to PM–AM conversion till the $(N-1)$th segment [which is to be added fictitiously at the beginning of the Nth segment], is given by

$$\chi(N-1,\,\omega) = \sum_{i=1}^{N-1} 2\,\sin[F(\omega)]\phi^{(i)}(0,\,\omega)L'_{N_{\rm eff}}\gamma P_o \quad (30)$$

where $L'_{N_{\rm eff}} = (1-e^{-\alpha L'_N})/\alpha$.

In order to find out $\phi^{(i)}(0,\,\omega)$, we follow a perturbative approach. In the zeroth-order approximation we neglect the term $\chi(N-1,\,\omega)$ and approximate (29) as

$$\phi_N(L_N,\,\omega) \approx H_{DS}^{(N)}(L_N,\,\omega)\phi_{N-1}(L_{N-1},\,\omega). \quad (31)$$

Hence, in the zeroth-order approximation

$$\phi_i(0,\,\omega) = H_{DS,\,i,\,0}(\omega)\phi_1(0,\,\omega) \quad (32)$$

where the zeroth-order transfer function is given by

$$H_{DS,\,i,\,0}(\omega) = \prod_{k=1}^{N} H_D(L_k,\,\omega)\left[1+2\gamma P_o I\left(L'_k,\,L_D^{(k)},\,\omega\right)\right]. \quad (33)$$

Now $\phi_i(0,\,\omega)$ as obtained in (32) is used in (30) to obtain the correction term of the transfer function for the N segment case as

$$\Delta H_{DS,\,N}^1(\omega) = 2\gamma P_o \sum_{k=2}^{N} H_D^{(k)} \cdot \left[\sum_{i=1}^{k-1} 2\,\sin[F(L_i,\,\omega)]H_{DS,\,i-1,\,0}(\omega)\gamma P'_o L'_{k_{\rm eff}}\right]. \quad (34)$$

Combining (33) and (34) and applying linear phase approximation [8], we obtain the effective impulse response $h(t)$ for the cascaded links as

$$h(t) = \text{Re}\left[F^{-1}\left[H_{DS,N,0}(\omega)+\Delta H_{DS,\,N}^1(\omega)\right]\right]. \quad (35)$$

D. Analysis of Dispersion Compensated System by Perturbation Method

Equations (33) and (34) are useful equations for the design of dispersion compensated (DC) angle modulated system. For a DC system

$$H_{DS,\,i,\,0}(\omega) = \prod_{k=1}^{N}\left[1+2\gamma P_o I\left(L'_k,\,L_D^{(k)},\,\omega\right)\right]$$

because $\prod_{k=1}^{N} H_D(L_k,\,\omega) = 1$ due to the fulfillment of the condition $\sum \beta_2^k L_k = 0$. Hence, keeping only the first-order term in γP_0, (33) is approximated to

$$H_{DS,\,i,\,0}^{\rm DC}(\omega) \approx 1+\Xi(i,\,\omega) \quad (36)$$

where

$$\Xi(N,\,\omega) = \sum_{k=1}^{N}\left[2\gamma P_o I\left(L'_k,\,L_D^{(k)},\,\omega\right)\right].$$

Utilizing (36), the transfer function for a DC system can be obtained as

$$H_{\rm DC}(\omega) = 1+\Delta H_{DS,\,N}^1(\omega)+\Xi(\omega). \quad (37)$$

Using (33), for small $F(\omega,\,L_i)$, (34) can be further approximated as

$$\Delta H_{DS,\,N}^1(\omega) = 2\gamma P_o \sum_{k=2}^{N} H_D^{(k)}(\omega) \cdot \left[\sum_{i=1}^{k-1}\{2\,\sin[F(\omega,\,L_i)]\} + \sum_{i=1}^{k-1}\{2\,\sin[F(\omega,\,L_i)]\}\{\Xi(i,\,\omega)\}\right] \cdot (\gamma P'_o L'_{k_{\rm eff}})]. \quad (38)$$

Now, for a distributed compensation if all $L_i = L$ and $\beta_2^k = -\beta_2^{k+1}$, then $\sum_{i=1}^{k-1} 2\,\sin[F(L_i)\omega^2] = 0$. This implies that for a distributed compensation scheme, PM–AM conversion is also suppressed thereby explaining the fact that in an angle modulated system, the distributed compensation is superior to post- or precompensation (Fig. 5). Among the post- and precompensation, (38) suggests that postcompensation should be preferred over precompensation due to existence of $H_D^{(k)}$ term in the outer sum; a high value of $F_i(L_i)$ for lower value of i [i.e., for precompensation scheme, $i = 1$] will create comparatively larger distortion (Fig. 7). The accuracy of the perturbative method decreases with an increase in the nonlinear effect. This is because of the fact that in strong nonlinear region $\Delta H(z,\,\omega)$ can not be treated as a perturbative element. Due to this difficulty, we present a more accurate method following transfer matrix approach.

E. The Matrix Method

Utilizing the $\lim_{z\to 0} \boldsymbol{o}(z) = \alpha' z^2$ where α' is a constant, we can establish the relation between the vectors $\xi(z)$ and $\xi(z+\Delta z)$ through the development of an infinitesimal evolution operator $A(z+\Delta z,\,z)$ using (13)

$$\xi(z+\Delta z) = \boldsymbol{A}(z+\Delta z,\,z)\xi(z). \quad (39)$$

The evolution operator $\boldsymbol{A}(z+\Delta z,\,z) = \boldsymbol{N}(z,\,\omega)\boldsymbol{D}(z,\,\omega)$ can be expressed as

$$\boldsymbol{A}(z+\Delta z) = \mathbf{1}+\boldsymbol{\Delta M^1}(z,\,\omega)\,dz+\cdots \quad (40)$$

where the matrix $\Delta M^1(z,\,\omega)$ is the generator of the infinitesimal transformation $\xi(z)\to\xi(z+\Delta z)$ and is expressed as

$$\boldsymbol{\Delta M^1}(z_0,\,\omega) = \begin{pmatrix} 0 & \left(\gamma - \dfrac{\omega^2\beta_2}{2P_0 e^{-\alpha z}}\right) \\ 2P_o e^{-\alpha z}\omega^2\beta_2 & 0 \end{pmatrix} \quad (41)$$

and $\mathbf{1}$ is the unity matrix, P_0 is the average input power level. Hence, the differential evolution of the evolution matrix $A(z,\,z_0)$ can be obtained from (40)

$$\frac{d\boldsymbol{A}(\boldsymbol{z},\,\boldsymbol{z}_0)}{dz} = \boldsymbol{\Delta M^1}(z,\,\omega)\boldsymbol{A}(z,\,z_0). \quad (42)$$

The solution to this equation over a fiber length L can be written as

$$\boldsymbol{A}(L,\,0,\,\omega) = \mathbf{1}+\int_{z=0}^{z=L}\boldsymbol{\Delta M^1}(z,\,\omega)A(z,\,0,\,\omega)\,dz. \quad (43)$$

Hence, $A(L, 0, \omega)$ is the effective transfer function of the system. Another useful form of $A(L, 0, \omega)$ for computation is given by

$$\boldsymbol{A}(L, 0, \omega) \approx \exp\left[\int_{z=0}^{L} \boldsymbol{\Delta M^1}(z, \omega)\, dz\right]. \tag{44}$$

Bearing an analogy with the Hamilton–Jacoby theory [14], we define an action integral $S(L, \omega) = \int_{z=0}^{L} \boldsymbol{\Delta M^1}(z, \omega)\, dz$ which will be proved to be useful in analyzing the dispersion compensated system in subsequent sections. Finally, the output vector is obtained as the solution of (39):

$$\xi(\omega, L) = e^{S(L, \omega)}\xi(\omega, 0). \tag{45}$$

Equation (45) now can be employed to find out the effective phase impulse response of a cascaded multisegment fiber optic link employing an angle modulated system. If L_i denote the length of the ith segment and g_i is the gain of the ith amplifier, then for an N cascaded segments, we have

$$\begin{pmatrix} \phi_{\text{out}}(\omega) \\ \zeta_{\text{out}}(\omega) \end{pmatrix} = B_{\text{SPM}}(N, \omega) \begin{pmatrix} \phi_{\text{in}}(\omega) \\ \zeta_{\text{in}}(\omega) \end{pmatrix} \tag{46}$$

where the transfer matrix

$$B_{\text{SPM}}(N, \omega) = \boldsymbol{G_N} e^{S_N(L_N, \omega)} \cdots \mathrm{G}_{\boldsymbol{1}} e^{S_1(L_1, \omega)} \tag{47}$$

where the gain matrix $\boldsymbol{G_i}$ is given as

$$\boldsymbol{G_i} = \begin{pmatrix} 1 & 0 \\ 0 & g_i \end{pmatrix} \tag{48}$$

and g_i is the gain of the ith amplifier.

If the relative intensity noise of the transmitting laser is assumed to be absent [i.e., $\xi_{\text{in}}(\omega) = 0$], one can obtain from (46) the desired simplified relation

$$\phi_{\text{out}}(\omega) = H_{\text{fiber}}(\omega)\phi_{\text{in}}(\omega) \tag{49}$$

with

$$h(t) = \text{Re}\left[F^{-1}[H_{\text{fiber}}(w)]\right] = \text{Re}\left[F^{-1}B_{\text{SPM}}^{11}(N, \omega)\right] \tag{50}$$

and

$$B_{\text{SPM}}(N, \omega) = \begin{pmatrix} B_{\text{SPM}}^{11} & B_{\text{SPM}}^{12} \\ B_{\text{SPM}}^{21} & B_{\text{SPM}}^{22} \end{pmatrix}. \tag{51}$$

F. Analysis of Dispersion Compensated System by Matrix Method

For a realistic system design $\beta_2 L\omega^2$ can be considered to be small enough so that one can write

$$\begin{aligned} \left[e^{\boldsymbol{S}(L, \omega)}, \boldsymbol{G}\right] &= [\{\boldsymbol{1} + \boldsymbol{S}(\boldsymbol{L}, \omega)\}, \boldsymbol{G}] \\ &= [\boldsymbol{S}(L, \omega), \boldsymbol{G}] \\ &= \alpha(\beta_2 L\omega^2) \end{aligned} \tag{52}$$

where α is a constant matrix. Extending this operation to the higher order commutation relationship it turns out

$$\left[e^{\boldsymbol{S}(L, \omega)} \cdots \left[_{(r\text{th bracket})} e^{\boldsymbol{S}(L, \omega)}, \boldsymbol{G}\right]\right] = \alpha_r(\beta_2 L\omega^2)^r \tag{53}$$

where α_r is a constant matrix and rth bracket indicates rth-order commutation bracket. Rearranging (47) (see the Appendix) and keeping only the first-order commutation brackets, one finally obtains (see the Appendix)

$$B_{\text{SPM}}(N, \omega) = B_0(\omega) + \Delta B_0(\omega) \tag{54}$$

where

$$B_0(\omega) = \mathrm{G}_{\boldsymbol{N}} \cdots \boldsymbol{G_1} e^{\sum_{j=1}^{N} \boldsymbol{S_j}} \tag{55}$$

and

$$\Delta B_0(\omega) = \sum_{r=1}^{N-1} \left(\sum_{k=2}^{N} \left(\prod_{j=\{l, m\}: j\neq r}^{N} \boldsymbol{G_j} \left[e^{\boldsymbol{S_k}}, \boldsymbol{G_r}\right] \prod_{l=m, q: l\neq k}^{N} e^{\boldsymbol{S_l}} \right) \right) \tag{56}$$

$\prod_{j=\{l, m\}: j\neq r}^{N} \boldsymbol{G_j}[e^{\boldsymbol{S_k}}, \boldsymbol{G_r}]$ is the product of all possible permutation of m, q. With the approximation $e^{\boldsymbol{S_k}} \approx \boldsymbol{1} + \boldsymbol{s_k}$ and (52), (56) is reduced to

$$\Delta B_0(\omega) = \sum_{r=1}^{N-1} \left(\sum_{k=2}^{N} \left(\boldsymbol{G_N} \cdots \boldsymbol{G_{k+1}} \alpha' \left[\beta_{\boldsymbol{2}}^{(\boldsymbol{k})} \omega^{\boldsymbol{2}}\right] \boldsymbol{G_{k-1}} \boldsymbol{G_j} \right) \right). \tag{57}$$

In a distributed compensation scheme if all $L_i = L$ and $\beta_2^k = -\beta_2^{k+1}$, then $B_0(\omega) = \boldsymbol{G_N} \cdots \mathrm{G}_{\boldsymbol{1}}$ by virtue of $\sum \beta_2^k = 0$. Since $\zeta_{\text{in}}(\omega) = 0$ no phase distortion is introduced from the term $B_0(\omega)$. This indicates that for a distributed compensation scheme the PM–AM conversion is also suppressed. For pre and postcompensation schemes, the term $B_0(\omega)$ will be the dominating term in the phase distortion process. Hence we can conclude that for an angle-modulated system the distributed compensation is superior to either post- or precompensation. This fact has been further confirmed by the simulation studies (Fig. 5) Between the post- and precompensation schemes, (56) suggests that the postcompensation should be preferred to precompensation due to the existence of $[G_i, S_k]$ term. The term $\beta_2^{(k)}\omega^2$ will be multiplied $[N - k]$ times by the gain matrix and for a lower value of k (i.e., for precompensation $k = 1$) if $[G_i, S_k]$ takes the large value (as it will be the case for a lump compensation, because a high value of $\beta_2 L$ will be used for compensation), the contribution due to the term $\Delta B_0(\omega)$ will be comparatively higher than the case where the commutation bracket takes a large value at a high value of k (i.e., for postcompensation $k = N$). Physically, this means that if high PM–AM conversion takes place at the beginning, it will be amplified by all subsequent amplifiers and a high SPM phase will result due to the amplified PM–AM conversion. This fact has been further confirmed by simulation and theoretical studies (see Fig. 7).

G. ASE Noise Evaluation

The real part of the complex envelope of ASE noise $n(t)$ at the output of the nth amplifier can be expressed as following [16]:

$$\begin{aligned} \text{Re}[n(t)] = \sum_m &[\{a_{m,n} \cos(2\pi f_m t) + c_{m,n} \sin(2\pi f_m t)\} \\ &\cdot \cos(2\pi f_c t) + b_{m,n} \cos(2\pi f_m t) \\ &- d_{m,n} \sin(2\pi f_m)\} \sin(2\pi f_c t)] \end{aligned} \tag{58}$$

where $a_{m,n}$, $b_{m,n}$, $c_{m,n}$, and $d_{m,n}$ are the Fourier coefficient of the inphase and quadrature component of the ASE noise generated from the nth amplifier and f_c is the optical carrier frequency. In a medium haul transmission, the noise envelope $n(t)$

evolves independently of the signal envelope because the effective coupling between the noise envelope and the signal envelope through the SPM-phase does not bring any significant correlation between them due the large signal to ASE noise ratio [6]. This fact has been confirmed by our simulation studies on the variance of phase distortion (Fig. 1) and penalty curves (Figs. 4 and 5). The coefficient $a_{m,n}$ and $b_{m,n}$ can be determined following [16]:

$$\begin{pmatrix} a_{m,n} \\ b_{m,n} \end{pmatrix} = \boldsymbol{M}(\omega) \begin{pmatrix} n_{a,i} \\ n_{b,i} \end{pmatrix} \tag{59}$$

where

$$\boldsymbol{M}(\omega) = \sum_{i=1}^{n} \begin{pmatrix} M_{11} & M_{12} \\ M_{21} & M_{22} \end{pmatrix} \tag{60}$$

where

$$M_{11} = \cos\Big(k\sqrt{\xi'(\xi'+\eta')L}\Big)$$
$$M_{12} = \sqrt{\xi'/(\xi'+\eta')}\,\sin\Big(k\sqrt{\xi'(\xi'+\eta')L}\Big)$$
$$M_{21} = \sqrt{\xi'/(\xi'+\eta')}\,\sin\Big(k\sqrt{\xi'(\xi'+\eta')L}\Big)$$

and

$$M_{22} = \cos\Big(k\sqrt{\xi'(\xi'+\eta')L}\Big)$$

where $k = n-i+1$, $n_{a,i}$, and $n_{b,i}$ are, respectively, the in-phase and the out of phase components of the ASE noise generated at the end of the ith amplifier, and $\langle n_{a,i}^2\rangle = \langle n_{b,i}^2\rangle = \langle n_o^2\rangle$ where $\langle n_o^2\rangle = 2n_{sp}(G-1)h\nu\Delta f$ and $\Delta f = f_m - f_{m-1}$, all the frequency components f_m have been assumed to be spaced with an equal interval of Δf. The quantities η' and ξ' are, respectively, given by $\xi' = \beta_2(2\pi f_m)^2/2$ and $\eta' = 2\gamma P_{av}$, where the $P_{av} = ((1-e^{-\alpha L})/L)P_o$. The other coefficients $c_{m,n}$ and $d_{m,n}$ can be determined exactly in the same way because of the symmetry in (34). With the resulting noise envelope and following [16], the phase noise due to ASE, as evolved in the presence of GVD and Kerr nonlinearity can be represented as

$$\theta_n'(t) = \frac{r_{\text{out}}(t)}{A_c}\,\sin\psi_n(t) \tag{61}$$

where

$r_{\text{out}}(t)$	is the noise envelope;
A_c	is the average signal envelope;
$\psi_n(t)$	is a random phase uniformly distributed between 0 and 2π.

H. Bit Error Rate Evaluation

The matrix/perturbation method provides an useful way of determining the phase of the complex signal at the fiber end by convolving the input phase with the equivalent phase response of the nonlinear fiber. This readily allows the theoretical evaluation of the transmission penalty of a CPFSK system considered in the present case.

For a heterodyne CPFSK system using delay demodulation receiver with a delay time $\tau = T/2m$, T is the bit duration, m is the modulation index and knowing the fiber phase impulse response $h(t)$, the signal phase distortion, for a "mark" transmitted, due to GVD, SPM, and ASE noise at a sampling time t_0 can be written as [18]

$$\begin{aligned}\Delta\phi(t) &= \Big[-\frac{\pi}{2} + \frac{\pi}{2}\,q(t_o)\Big] + \frac{\pi}{2}\sum_{k\neq 0} a_k q(t_o - kT) + \Delta\theta_n(t_o) \\ &= \Delta\alpha_0 + \xi + \Delta\theta_n(t_0)\end{aligned} \tag{62}$$

where $a_k = \pm$ represents the information bits, $q(t) = (1/\tau)\int_{t-\tau}^{t} g(t')\,dt'$ and $g(t) = \text{Re}[p(t)\otimes h(t)\otimes h_{IF}(t)]$, where

$h_{IF}(t)$	is the low-pass impulse response of the IF filter,
$p(t)$	is the elementary pulse shape of the NRZ data and
$\Delta\theta_n(t)$	is the phase distortion due to ASE noise and receiver noise,
$\otimes$	denotes convolution.

The bit-error rate (BER) probability can be evaluated following [18] utilizing the Gauss quadrature rule as

$$\text{BER} = \int_{-\infty}^{\infty} P(e/\xi)p(\xi)\,d\xi \tag{63}$$

where

$$P(e/\xi) = \frac{1}{2} - \frac{1}{2}\rho e^{-\rho}\sum_{n}\frac{(-1)^n}{2n+1}\Big[I_n\Big(\frac{\rho}{2}\Big) + I_{n+1}\Big(\frac{\rho}{2}\Big)\Big]^2 \cdot \cos[(2n+1)(\Delta\alpha_0+\xi)]$$

and ρ is the IF SNR, $I_n(x)$ is the modified Bessel function of first kind and order n.

I. Electronic Compensation

The transmission penalty due to GVD and other nonlinear impairment for a coherent optical system can be substantially reduced by electronic dispersion equalization at the IF domain [18]. With a microstrip delay equalizer $H_{eq}(\omega)$ placed at the IF stage of the receiver, the linear phase approximation directly allows to modify (49) to

$$\phi_{\text{out}}(\omega) = H_{eq}(\omega)H_{\text{fiber}}(\omega)\phi_{\text{in}}(\omega) \tag{64}$$

where

$$H_{eq}(\omega) = e^{jF_{eql}\omega^2}$$
$$F_{eql} = \frac{l\sqrt{3h(\epsilon_r-1)/2}\,Gf_o}{\epsilon_{\text{eff}}f_p}$$

l, w, and h represent the length, width, and thickness, respectively, of the microstrip equalizer

$$\epsilon_{\text{eff}} = \frac{\epsilon_r+1}{2} + \frac{\epsilon_r-1}{2}\Big(1+12\,\frac{h}{w}\Big)^{-0.5}$$

$f_p = Z_o/8\pi h$, f_o is the IF frequency and $G = 0.6\times 0.0009Z_o$ [19].

III. Simulation Technique

Numerical SSF method has been used to obtain the $\phi_{\text{out}}(t)$ of the CPFSK signal with the input phase obtained from $2^7 - 1$ NRZ bit pattern. The ASE noise of the ith amplifier has been simulated from its noise variance $\sigma_{\text{ASE}}^2 = 2n_{sp}(g^{(i)}-1)h\nu$ where n_{sp} is the spontaneous noise emission factor and $h\nu$ is the photon energy. The Q-value simulation has been carried out by assuming that the probability density function (pdf) of the phase distortion process of $\sin(\Delta\phi_{\text{out}}(t))$, is a conditional Gaussian

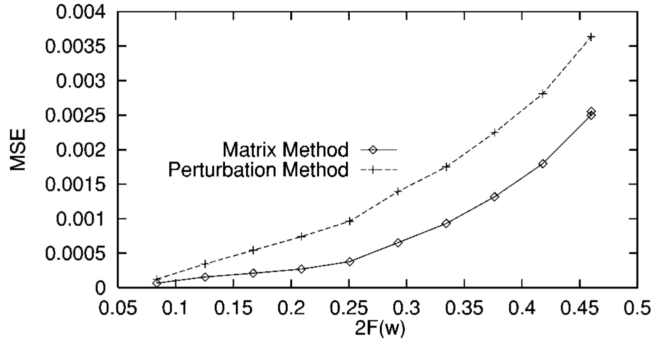

Fig. 2. Comparison of the MSE between the simulated phase and theoretically obtained phase. $\beta_2 = 20.9$ ps^2/km, bit-rate, $B = 10$ Gb/s, $P_0 = 7$ dBm.

distribution, since the closure of the eye pattern is mostly governed by the data sequences 101 and 010 [6]. Hence, assuming that the conditional pdf $p(\Delta\phi/101)$ and $p(\Delta\phi/010)$ follow a Gaussian distribution (Fig. 10), the bit error rate is evaluated as

$$\text{BER} = P_{(101)}P(e/101) + P_{(010)}P(e/010) \tag{65}$$

where $P_{(010)}$ and $P_{(101)}$ are the probability of the occurrence of the bit patterns 010, 101, respectively, and both are equal to 1/8. Each conditional error probability is given by $P(e/101) = P(e/010) = (1/2)\,\text{erfc}(Q/\sqrt{2})$, where $Q = (s_1 - s_0)/(\sigma_1 + \sigma_0)$, where s_1, σ_1^2 and s_0, σ_0^2 are the mean and the variance of the sample values corresponding to the 1th and 0th bit, respectively.

It is to be noted that the output envelope can be also obtained employing matrix and perturbation methods Both these methods are found to provide a computational advantage by approximately a factor of M compared to SSF method as noted in the following. If N is the number of samples in the timing-window and M is the number of steps used in SSF/matrix method, the computational requirements are

$$T_{\text{BPM}} = 2MN(\log_2 N + 1)[2M \text{ FFT } + 2N \text{ complex multiplication at each step}]$$

$$T_{\text{Matrix}} = 2N(\log_2 N + 4M)[2 \text{ FFT } + 8N \text{ complex multiplication at each step}]$$

$$T_{\text{Perturbation}} = N(2\log_2 N + 1)[2 \text{ FFT} + N \text{ complex multiplication}].$$

IV. Results

The validity of both perturbation method and the more accurate matrix method in determining the output phase (i.e., the output phase and the phase distortion) at the end of the transmission link is established by depicting in Fig. 2 the (MSE) between the simulated phase and the theoretically obtained output phase for an input CPFSK signal driven by a $2^7 - 1$ NRZ bit-sequence with $\beta_2 = 20.9$ ps^2/km (SMF fiber), bit-rate $= 10$ Gb/s and a power level of 7 dBm. The system under consideration is depicted in Fig. 3. As noticed, both methods provide reasonably good estimates of the phase distortion with the matrix method being more accurate. Both the methods are computationally less time consuming than the numerical SSF method. Next, we establish the validity of the independent evolution of the signal and the ASE noise in a nonlinear transmission fiber.

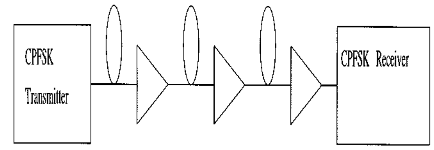

Fig. 3. Variance of phase distortion process versus the repeater output power due to (a) ASE, (b) GVD and SPM (theory), and (c) GVD, SPM, and ASE (simulation).

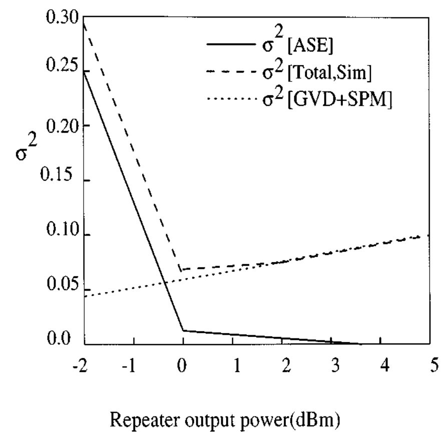

Fig. 4. Block diagram of a repeatered CPFSK transmission system.

Fig. 4 depicts the variance of the phase distortion process as contributed by the phase noise due to ASE and due to GVD/SPM for a 2.5-Gb/s multisegment CPFSK transmission system with the system parameters: $\alpha = 0.2$ dB/km, $\gamma = 0.0235$ mw^{-1}km^{-1}, $\lambda = 1550$ nm, $\beta_2 = 2$ ps^2/km (DSF fiber) and each $L_k = 50$ km. The near equality of σ_ϕ^2 (total) obtained by simulation with the sum $\sigma_\phi^2(\text{ASE}) + \sigma_\phi^2(\text{GVD} + \text{SPM})$ obtained from the theory clearly establishes the assumption of independence used in the theoretical analysis.

The theoretical BER evaluation has been carried out for the system depicted in Fig. 3 and the results are shown in Fig. 5 for a 10-segment, CPFSK link (a segment length $L_k = 100$ km) with a total dispersion of 57 ps/nm. For comparison the BER for a back to back system is also indicated. The penalty versus the input power for the above system as obtained theoretically, experimentally [20] and by Q-value simulation is shown in Fig. 6. The theoretical results are found to match very well with the experimental results justifying the approximations made in the present theory. The slight overestimation of the Q-value simulation is due to the simplified assumption of Gaussian distribution of the output phase distortion statistics. Fig. 7 shows the conditional PDF of the $P(\Delta\phi/010)$ and its corresponding Gaussian closure in normalized form. This shows that Gaussian PDF has a larger tail than the actual PDF as obtained from the simulation of CPFSK phase corresponding to $8 \times [2^8 - 1]$ bit pattern, indicating that the Q-value simulation exhibits a higher penalty than the analytical method. Fig. 8 depicts the penalty versus repeater output power (details of the system are available in [19]) of a multisegment CPFSK system with dispersion equalizer at the IF level. The theoretical penalty estimates are found to agree very well with the reported experimental results [18].

Fig. 9 depicts a comparison between the performance of pre- and postdispersion compensation schemes (placement of

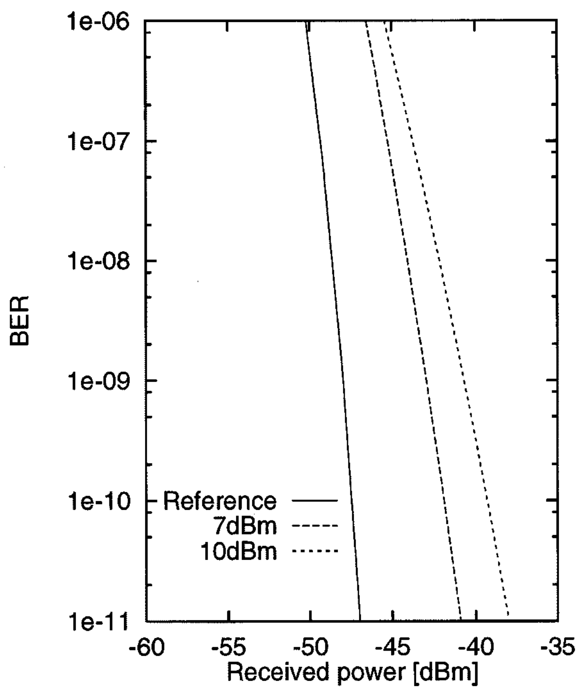

Fig. 5. BER curve as obtained from the matrix method.

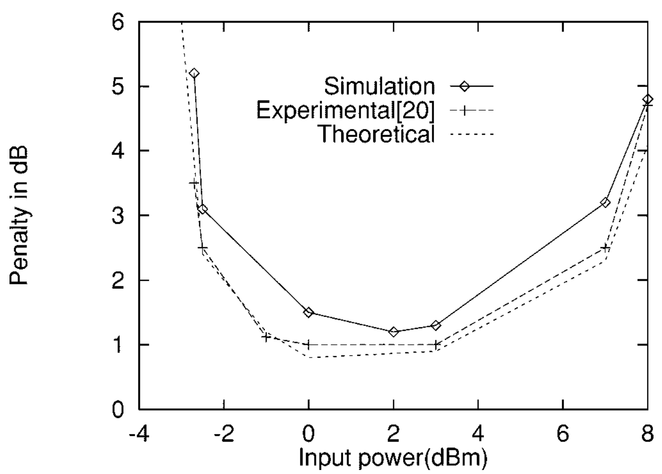

Fig. 6. Transmission penalty versus input power (dBm) in an uncompensated CPFSK system.

dispersion compensating fiber before and after the transmission fiber respectively) in achieving a reduced system penalty using the matrix method and the numerical SSF simulation for the same transmission system as above except that the dispersion coefficient of each DSF segment is 2 ps/km·nm. As noticed, both compensation schemes behave almost similarly in the ASE dominated region and at a higher power level, the precompensation produces more GVD induced SPM penalty and the simulation results are found to match very closely with those of theory. The post-compensation is found to perform better than the precompensation. Fig. 10 shows a comparison of a distributed compensated scheme with the above mentioned postcompensation scheme in the absence of ASE noise. For distributed compensation, DSF fibers of ± 2 ps/km·nm are used in alternate segment keeping other specifications same as that

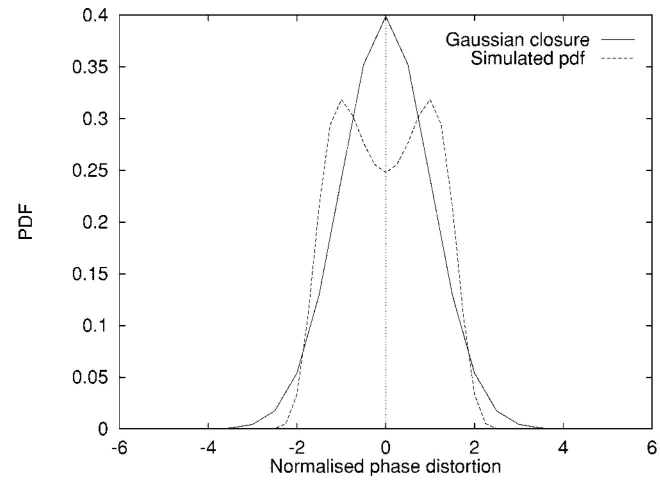

Fig. 7. Comparison of Gaussian closure and actual conditional PDF of $p(\Delta\Phi/010)$ as obtained through histogram.

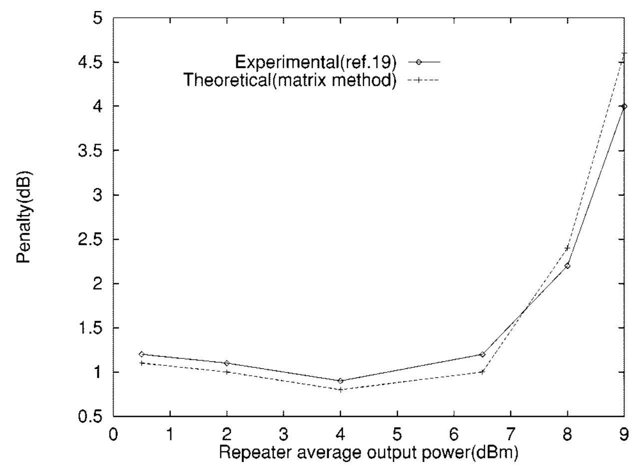

Fig. 8. Transmission penalty in a CPFSK system with electronic dispersion equalization.

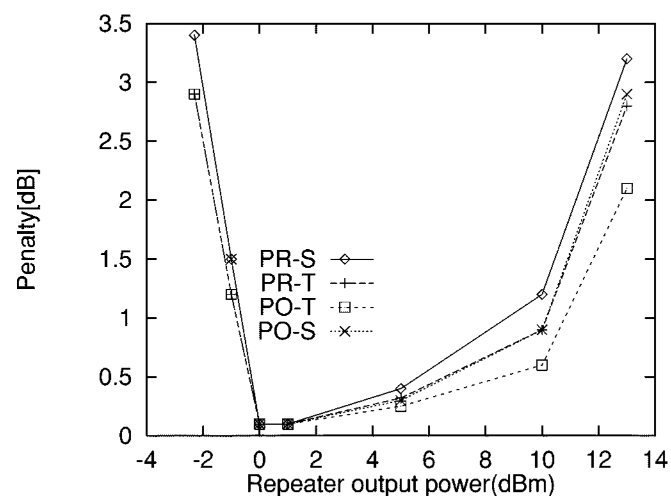

Fig. 9. Power penalty versus repeater output power in a 2.5-Gb/s CPFSK transmission link with pre- and postdispersion compensation.

of postcompensation. As predicted theoretically, distributed compensation is found to perform better than the postcompensation.

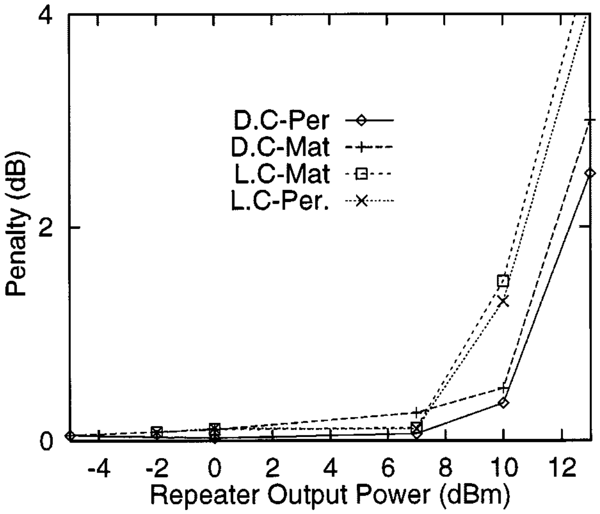

Fig. 10. System performance of 20 segment CPFSK link (in the absence of ASE): L.C = lump compensation, D.C = distributed compensation, Mat. = matrix method, Per. = perturbation theory.

V. Conclusion

Two useful analytical methods by perturbation theory and matrix formalism are developed which allow direct evaluation of BER of a repeatered coherent CPFSK transmission system impaired by GVD, SPM, and ASE noise. Both have been developed from the analogy of mathematical framework of time dependent Schroedinger equation in quantum mechanics and are analytically useful for the prediction of the performance of different kind of dispersion compensated systems. The theories are also applicable to electronic dispersion equalization management. The perturbation method is computationally less time consuming which makes it a suitable method for the analysis of weak nonlinear effects in large scale optical networks. The matrix method is applicable to both situation of weak and strong nonlinear effect and also consumes much less computation time compared to SSF method in long cascaded segme

The developed analytical theories can be applied in a straightforward manner to study the joint impact of GVD, SPM, and ASE noise in other angle-modulated systems such as PSK, DPSK, etc. Finally, the present theoretical methodology can also be extended in the larger practical environment of IM–DD systems and this is presently being carried out.

Appendix

Let a matrix $\boldsymbol{D}$ be represented by

$$\boldsymbol{D} = \boldsymbol{C_N C_{N-1}} \cdots \boldsymbol{C_2 C_1} \tag{66}$$

where $\boldsymbol{C_r} = \boldsymbol{A_r B_r}$, $[\boldsymbol{A_r} = \boldsymbol{G_r}, \boldsymbol{B_r} = \exp(\boldsymbol{S_r})]$. Utilizing the Identity $\boldsymbol{AB} = \boldsymbol{BA} + [\boldsymbol{A}, \boldsymbol{B}]$, we obtain

$$\begin{aligned}\boldsymbol{A_2B_2A_1B_1} &= \boldsymbol{A_2A_1B_2B_1} + \boldsymbol{A_2}[\boldsymbol{B_2}, \boldsymbol{A_1}]\boldsymbol{B_1} \\ &= \boldsymbol{E_2F_2} + \boldsymbol{A_2}[\boldsymbol{B_2}, \boldsymbol{A_1}]\boldsymbol{B_1}\end{aligned} \tag{67}$$

with $\boldsymbol{E_2} = \boldsymbol{A_2A_1}$ and $\boldsymbol{F_2} = \boldsymbol{B_2B_1}$. Similarly $\boldsymbol{A_4B_4A_3B_3} = \boldsymbol{E_4F_4} + \boldsymbol{A_4}[\boldsymbol{B_4}, \boldsymbol{A_3}]\boldsymbol{B_3}$ with $\boldsymbol{E_4} = \boldsymbol{A_4A_3}$ and $\boldsymbol{F_4} = \boldsymbol{B_4B_3}$. Hence

$$\begin{aligned}&\boldsymbol{A_4B_4A_3B_3A_2B_2A_1B_1} \\ &\quad = (\boldsymbol{E_4F_4} + \boldsymbol{A_4}[\boldsymbol{B_4}, \boldsymbol{A_3}]\boldsymbol{B_3})(\boldsymbol{E_2F_2} + \boldsymbol{A_2}[\boldsymbol{B_2}, \boldsymbol{A_1}]\boldsymbol{B_1}) \\ &\quad = \boldsymbol{E_4F_4E_2F_2} + \boldsymbol{A_4}[\boldsymbol{B_4}, \boldsymbol{A_3}]\boldsymbol{B_3E_2F_2} \\ &\qquad + \boldsymbol{E_4F_4A_2}[\boldsymbol{B_2}, \boldsymbol{A_1}]\boldsymbol{B_1} + \boldsymbol{A_4}[\boldsymbol{B_4}, \boldsymbol{A_3}] \\ &\qquad \cdot \boldsymbol{B_3A_2}[\boldsymbol{B_2}, \boldsymbol{A_1}]\boldsymbol{B_1}.\end{aligned} \tag{68}$$

Matrix elements of $\boldsymbol{A_4}[\boldsymbol{B_4}, \boldsymbol{A_3}]\boldsymbol{B_3E_2F_2}$ and $\boldsymbol{A_4}[\boldsymbol{B_4}, \boldsymbol{A_3}]\boldsymbol{B_3A_2}[\boldsymbol{B_2}, \boldsymbol{A_1}]\boldsymbol{B_1}$ are of the the order $F(\omega)$ and $F^2(\omega)$, respectively. Since $F(\omega) \ll 1$ and $F^2(\omega) \ll F(\omega)$, neglecting the terms involving higher orders of $F(\omega)$, (68) is rewritten as

$$\begin{aligned}&\boldsymbol{A_4B_4A_3B_3A_2B_2A_1B_1} \\ &\quad = (\boldsymbol{E_4F_4} + \boldsymbol{A_4}[\boldsymbol{B_4}, \boldsymbol{A_3}]\boldsymbol{B_3})(\boldsymbol{E_2F_2} + \boldsymbol{A_2}[\boldsymbol{B_2}, \boldsymbol{A_1}]\boldsymbol{B_1}) \\ &\quad = \boldsymbol{E_4F_4E_2F_2} + \boldsymbol{A_4}[\boldsymbol{B_4}, \boldsymbol{A_3}]\boldsymbol{B_3E_2F_2} \\ &\qquad + \boldsymbol{E_4F_4A_2}[\boldsymbol{B_2}, \boldsymbol{A_1}]\boldsymbol{B_1}.\end{aligned} \tag{69}$$

Extending this operation $(N-1)$th time and adopting the same technique repeatedly

$$\begin{aligned}\boldsymbol{D} &= \boldsymbol{A_N} \cdots \boldsymbol{A_1B_N} \cdots \boldsymbol{B_1} \\ &\quad + \sum_{r=1}^{N-1}\left(\sum_{k=2}^{N}\left(\prod_{j=\{l,m\}:j\neq r}^{N} \boldsymbol{A_j}[\boldsymbol{B_k}, \boldsymbol{A_r}] \prod_{l=m,q:l\neq k}^{N} \boldsymbol{B_l}\right)\right).\end{aligned} \tag{70}$$

Acknowledgment

B. Pal would like to acknowledge the Council for Scientific and Industrial Research (CSIR), India, for providing the research fellowship to carry out this work. The authors are also grateful to the reviewers for providing useful feedback to improve the quality of the manuscript.

References

[1] M. J. Potasek, G. P. Agrawal, and S. C. Pinault, "Analytical and numerical study of pulse broadening in nonlinear dispersive optical fibers," *J. Opt. Soc. Amer. B*, vol. 3, pp. 205–211, 1986.

[2] N. Kikuchi and S. Sasaki, "Analytical evaluation technique of self-phase modulation effect on the performance of cascaded optical amplifier systems," *J. Lightwave Technol.*, vol. 13, pp. 868–878, 1995.

[3] G. P. Agrawal, *Nonlinear Fiber Optics*. New York: Academic, 1989.

[4] N. Takachio, S. Norimatsu, and K. Iwashita, "Optical PSK synchronous heterodyne detection transmission experiment using fiber chromatic dispersion equalization," *IEEE Photon. Technol. Lett.*, vol. 4, pp. 278–280, 1992.

[5] F. Matera and M. Settembre, "Performance of optical links with optical amplifiers," *Fiber Integr. Opt.*, vol. 15, pp. 89–107, 1996.

[6] S. Betti, G. D. Marchis, and E. Innone, *Coherent Optical Communication System*. New York: Wiley, 1995.

[7] E. Bedrosian and S. O. Rice, "Distortion and cross talk of linearly filtered angle modulated signals," *Proc. IEEE*, vol. 56, pp. 2–13, 1968.

[8] R. Gangopadhaya, S. P. Majumdar, B. Pal, and R. Dimuro, "Sensitivity penalty for direct detection CPFSK receiver due to laser phase noise and chromatic dispersion," *J. Optic. Commun.*, vol. 20, pp. 98–100, 1999.

[9] E. Forestieri, "PM/AM and AM/PM conversions in linear optical fibers," in *Optical Networking*. New York: Springer, 1999.

[10] J. Wang and K. Peterman, "Small signal analysis for dispersive optical fiber communication systems," *J. Lightwave Technol.*, vol. 10, pp. 96–100, 1992.

[11] G. H. Weiss and A. A. Maradudin, “The Baker–Hausdorff formula and a problem in crystal physics,” *J. Math. Phys.*, vol. 3, pp. 771–780, 1962.

[12] A. V. T. Cartaxo, B. Wedding, and W. Idler, “Influence of fiber nonlinearity on the phase noise to intensity noise conversion in fiber transmission: Theoretical and experimental analysis,” *J. Lightwave Tehnol.*, vol. 16, pp. 1187–1194, 1998.

[13] L. D. Landau and E. M. Lifshitz, *Quantum Mechanics*. New York: Pergamon, 1965.

[14] H. Goldstein, *Classical Mechanics*. New York, MA: Addison-Wesley, 1961.

[15] B. Pal, S. P. Majumdar, and R. Gangopadhyay, “Evaluation by matrix method heterodyne CPFSK transmission penalty due to GVD, SPM and ASE noise,” in *Proc.IEEE/LEOS Conf.*, FL, 1998.

[16] K. Kikuchi, “Enhancement of optical amplifier noise by nonlinear refractive index and group-velocity dispersion of optical fibers,” *IEEE Photon. Technol. Lett.*, vol. 5, pp. 221–223, 1993.

[17] A. B. Carlson, *Communication System*. New York: McGraw-Hill, 1986.

[18] S. P. Majumdar, R. Gangopadhyay, E. Forestieri, and G. Prati, “Sensitivity penalty for AMI-coded CPFSK in heterodyne delay demodulation receiver,” *IEEE Photon. Technol. Lett.*, vol. 7, pp. 1207–1209, 1995.

[19] S. Yamazaki, T. Ono, and T. Ogata, “Compensation for chromatic dispersion and nonlinear effect,” *J. Lightwave Technol.*, vol. 11, pp. 603–611, 1993.

[20] S. Yamazaki, K. Fukuchi, T. Ono, and T. Ogata, “Estimation on maximum transmission distance for 2.5 Gb/s coherent FDM optical repeater systems,” *IEEE Photon. Technol. Lett.*, vol. 5, pp. 534–536, 1993.

B. Pal, photograph and biography not available at the time of publication.

R. Gangopadhyay, photograph and biography not available at the time of publication.

G. Prati, photograph and biography not available at the time of publication.